Reliability Engineering and System Safety 237 (2023) 109361

Contents lists available at ScienceDirect

Reliability Engineering and System Safety

journal homepage: www.elsevier.com/locate/ress

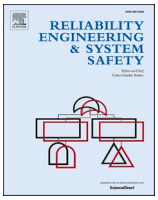

A power model considering initial battery state for remaining useful life prediction of lithium-ion batteries

Fanbing Meng [a], Fangfang Yang [b], Jun Yang [a,*], Min Xie [c,d]

[a] School of Reliability and Systems Engineering, Beihang University, Beijing, China
[b] School of Intelligent Systems Engineering, Sun Yat-sen University, Shenzhen, China
[c] Department of Advanced Design and System Engineering, City University of Hong Kong, Hong Kong SAR, China
[d] Shenzhen Research Institute, City University of Hong Kong, Shenzhen, China

ARTICLE INFO

Keywords:
Lithium-ion batteries
Degradation modeling
Power model
Remaining useful life prediction
Particle filter

ABSTRACT

Square-root-of-time model, constructed based on the growth of solid electrolyte interface layer, is an extensively-used semi-empirical model for remaining useful life (RUL) prediction of lithium-ion batteries. However, over the life cycle, the battery capacity degradation is not always under a linear relationship to the 1/2 power of the cycle number. In practice, its initial state, fresh or old, is rarely considered during RUL prediction. To address these concerns, a three-step mathematical transformation is proposed to improve the flexibility of square-root-of-time model. With initial battery state described by an initial cycle parameter, a power model is proposed to capture the battery capacity degradation. The parameter properties of proposed power model are then discussed in depth. Combining an offline parameter estimator and an online particle filter algorithm, a two-phase prediction framework is developed for onboard RUL prediction. Finally, a charge-discharge experiment is conducted, and its comprehensive experimental datasets of lithium iron phosphate batteries are analyzed. Results show that the proposed power model is superior to other existing degradation models on model fitting and extrapolation accuracy; and compared to the traditional square-root-of-time model, the RUL prediction accuracy is significantly improved.

1. Introduction

Lithium-ion batteries, as the main power storage devices of electric vehicles (EVs), have attracted more and more attention from the industry due to its advantages such as high energy density, high power density, and long lifetime [1]. As a battery's performance decreases over repeated usage, its remaining useful life (RUL) is of vital importance for the guidance of safe battery operation and effective performance optimization [2]. Accurate RUL information can also provide users ample forewarning of imminent battery failure and thus significantly reduce battery-power system risks.

1.1. Literature review

Existing methods for RUL prediction can be mainly divided into two categories: data-driven approach and model-based approach [3]. The data-driven approach regards the battery system as a black box and infer battery RUL or lifetime directly from features extracted from time, current, voltage, etc. [4,5]. Various methods have been proposed to model the nonlinear relationship between battery RUL and input features, including statistical analysis [6], signal processing [7], and artificial intelligence (AI) [8]. For example, Ardeshiri et al. [9] put forward a stacked bidirectional long short term memory algorithm to predict battery RULs through time-domain features. Xu et al. [10] employed a stacked denoising autoencoder algorithm to predict battery lifetime through a series of health features extracted from early cycle data. The data-driven approaches provide great flexibility and model-free characteristics, while its accuracy depends heavily on the quality and quantity of available training data. As training samples usually do not cover all possible operating conditions, the model-based approach, with self-correction property, is a better choice for applications with limited historical samples.

The model-based approaches establish mathematical models to describe the degradation behaviors of lithium-ion batteries, and then use filter techniques, such as particle filter (PF) [11], to update the model parameters and predict battery RUL accordingly. The mathematical

* Corresponding author.
E-mail address: tomyj2001@buaa.edu.cn (J. Yang).

https://doi.org/10.1016/j.ress.2023.109361
Received 6 July 2022; Received in revised form 4 April 2023; Accepted 3 May 2023
Available online 4 May 2023

models, as the key to the model-based approaches, can be divided into mechanism models, empirical models, and semi-empirical models [12]. The mechanism models focus on battery aging mechanisms and describe the battery physical and chemical reactions with arrays of equations. Darling et al. [13] estimated the reaction exchange current density and solid-state diffusion coefficient of lithium-ion batteries. Dai et al. [14] developed a capacity degradation model to depict the manganese dissolution of lithium-ion batteries. Xu et al. [15] proposed an Arrhenius temperature model and predicted the battery RUL via Wiener process. The aging mechanisms are usually diverse and require expert knowledge [16]. Typically, the mechanism models require intensive computations, and thus may be too slow to be employed for real-time online application [12].

As a comparison, the empirical models exploit historical data to predict battery future degradation behaviors without considering the physicochemical properties [17]. He et al. [18] put forward a two-term exponential model to model battery capacity degradation and predicted the RULs via Bayesian Monte Carlo and Dempster-Shafer theory. Micea et al. [19] proposed a quadratic polynomial model to fit the degradation data and predict battery RULs. Xing et al. [20] fused a polynomial model and a two-term exponential model to fit the capacity degradation and predict the RULs based on PF framework. Wang et al. [21] used a one-term exponential model to fit the capacity degradation path of the lithium-ion batteries. Yang et al. [22] put forward a two-term logarithmic model to capture the degradation curve of lithium-ion nickel manganese cobalt oxide cells and used a PF to predict battery RULs. With no consideration of physical or chemical mechanism basis, the empirical models may result in weakness of model interpretability and portability.

As a balance between mechanism models and empirical models, the semi-empirical models are built based on important internal mechanisms and weigh up the model accuracy, computation load, and model extrapolation [23]. For lithium-ion phosphate batteries, the major degradation mechanism is the loss of lithium inventory (LLI), which is caused by side reactions including impedance increase [24], lithium plating [25], SEI growth [26], etc.. Broussely et al. [27] found the growth of SEI layer follows a linear relationship to the square of time and proposed a square-root-of-time model to characterize the battery capacity degradation. By studying the relationship between coulombic efficiency (CE) and LLI, Yang et al. [12] put forward a CE model to describe the degradation of lithium-ion batteries. In between, the square-root-of-time model receives extensive attention from researchers and engineers due to its simple structure and good fitting ability. Based on the square-root-of-time model, Schmalstieg et al. [28] considered the effect of discharge rate and further put forward a two-stage aging model for lithium nickel manganese cobalt oxide batteries; Han et al. [29] considered the effect of temperature and proposed a temperature-based degradation model to estimate battery capacity.

1.2. Proposed methodology

Though the square-root-of-time model at present achieves acceptable prediction results, to the best of our knowledge, there are still two issues with its traditional structure. First, the assumption that the battery capacity is linear to the 1/2 power of the cycle number may not always be true. As reported in [12], the actual capacity degradation not only deviates from the square-root-of-time relationship but its rate also changes when the cycle number increases. Thus, the linear relationship to the 1/2 power of the cycle number is not good enough to accurately describe the whole-life capacity degradation. Second, the cycle number k in the test may not be the actual battery life cycle, i.e., the battery has been used or tested before the experiment. This common-seen problem, also illustrated in other work before (e.g. [30]), will influence the prediction accuracy. To address these two issues, in this paper, we improve the traditional square-root-of-time model by three-step mathematical transformation and put forward a power model to describe the whole-life capacity degradation. Specifically, the power exponent 1/2 in the square-root-of-time model is extended to a model parameter and a bias is then added to the cycle number. The model parameter properties are then theoretically discussed in depth. The fitting and extrapolation performance is verified with collected experimental degradation data and further compared with existing common-used degradation models.

To employ the proposed model for online RUL prediction, a PF is adopted in this paper. The PF plays an important role in the prediction of nonlinear and non-Gaussian systems [21,31], and has been widely employed for battery RUL prediction [20,32]. According to the Bayes theorem, the prior distribution and observed data directly decide the posterior distribution results, which means the choice of prior distribution plays an essential role in the prediction result. As the prior distribution in PF is reflected in the determination of initial parameter, an offline parameter estimator is proposed to determine the initial model parameter. The output of offline estimator is used as the input of PF algorithm, which improves the effectiveness of traditional PF algorithm. The performance of proposed method on RUL prediction is then investigated and compared with the square-root-of-time model and CE model. Results show that the RUL prediction based on the proposed method has better accuracy than these two models.

The rest of this paper is organized as follows: Section 2 introduces the proposed degradation model. Section 3 presents a two-phase RUL prediction method based on offline parameter estimator and online PF algorithm. Section 4 gives the experimental results of proposed method on both modeling and RUL prediction. Finally, Section 5 concludes the whole work.

2. Capacity degradation model

Based on the common-used square-root-of-time model, a new power model is proposed in this section. To verify its performance on degradation modeling and RUL prediction, six representative degradation models are shortly reviewed in Section 2.2.

2.1. Proposed power model

(1) **Original square-root-of-time model**

The square-root-of-time model assumes the increase of the SEI film thickness is proportional to the square root of time and further uses the thickening of SEI film to model the loss of lithium inventory. The mathematical expression of this model is denoted as

$$Y_k = ak^{1/2} + b, \tag{1}$$

where a and b are unknown parameters of this model.

(2) **Proposed power model**

The pros and cons of square-root-of-time model have been discussed previously. To address the two major concerns on the degradation rate and initial cycle, the traditional square-root-of-time model is improved by three steps as follows:

Step 1: Extend the power

To address the first concern, we extend the power exponent 1/2 in the square-root-of-time model to an intermediate variable parameter c_0:

$$Y_k = ak^{1/2} + b \rightarrow Y_k = a_0 k^{c_0} + b_0, \tag{2}$$

where a_0 and b_0 denote the intermediate variables to substitute variables a and b. Based on the fitting parameter c_0, the improved model can adapt to the degradation curve with different rates.

Step 2: Introduce the parameter considering the initial state

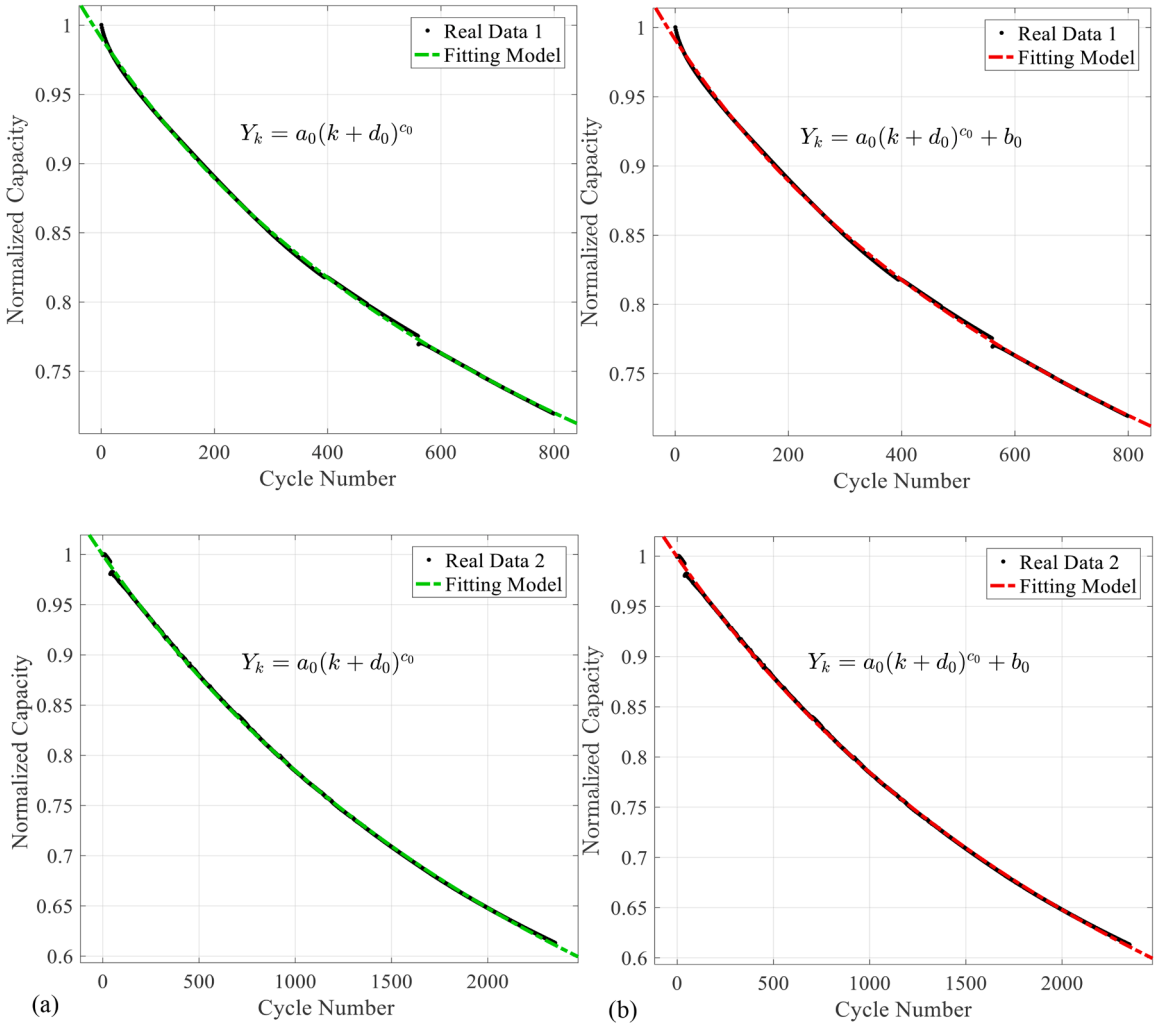

Fig. 1. Fitting comparison between $Y_k = a_0(k+d_0)^{c_0}$ and $Y_k = a_0(k+d_0)^{c_0} + b_0$ on (a) real data1 and (b) real data 2.

To address the second concern, an intermediate parameter d_0 is introduced to describe the real cycle number $k + d_0$:

$$Y_k = a_0 k^{c_0} + b_0 \rightarrow Y_k = a_0(k+d_0)^{c_0} + b_0. \tag{3}$$

The real cycle number $k + d_0$ can not only consider the cycle number before the experiment but also consider the battery difference in the initial state.

Step 3: Eliminate the intercept parameter

This step is devoted to eliminating parameter b_0 in Eq. (3). This elimination is supported by three reasons: 1) After fitting real degradation data in Fig. 1-2 and Tables 1-2, we found parameter b_0 in Eq. (3) has little effect on fitting results including the sum of squared errors (SSE), R-square, adjusted R-square (Adj. R-square) and RMSE. 2) Theoretically, parameter b_0 indicates the influence of some environmental and noise factors on the battery capacity and cycle number k can compensate the capacity influence. Since we introduce parameter d_0 in Step 2, the change of parameter d_0 can be effectively reflected on cycle number b_0. Thus, the influence of capacity can be indirectly compensated by cycle number b_0. Of course, besides cycle number b_0, linear factor parameter a and nonlinear factor parameter b will also affect the accurate fitting. 3) After eliminating the parameter b_0, the mathematical form becomes concise and can avoid the overfitting problem when the sample size is limited. Furthermore, Lin et al. [30] also empirically provided the same mathematical form for different scenarios and methods without the intercept parameter. In his paper, this mathematical form is served as the scale parameter of the gamma process, and the scale parameter of the gamma process depicts the degradation quantity of each jump in the stochastic process. However, in this paper, the mathematical form is derived and introduced to depict the global degradation path. Although the application scenarios and methods are totally different in Lin's paper and this work, the mathematical form is accidently consistent, which indicates the strong fitting and prediction ability of this mathematical form. Based on the above reasons, we eliminate parameter b_0 and get Eq. (4):

$$Y_k = a_0(k+d_0)^{c_0} + b_0 \rightarrow Y_k = a_0(k+d_0)^{c_0}. \tag{4}$$

Finally, substitute the intermediate variables a_0, d_0 and c_0 with new parameters a, b, and c. The capacity degradation model we put forward in this paper can be re-organized as

$$Y_k = a_0(k+d_0)^{c_0} \xleftrightarrow{\text{re-organize}} Y_k = a(k+b)^c, \tag{5}$$

where new parameters a, b, c respectively denote the scale parameter, location parameter, and shape parameter of the proposed model. The above procedure finishes the transformation from the square-root-of-time model $Y_k = ak^{1/2} + b$ to the proposed model $Y_k = a(k+b)^c$.

(3) **Discussion on model parameters**

Compared with square-root-of-time model, the proposed model in

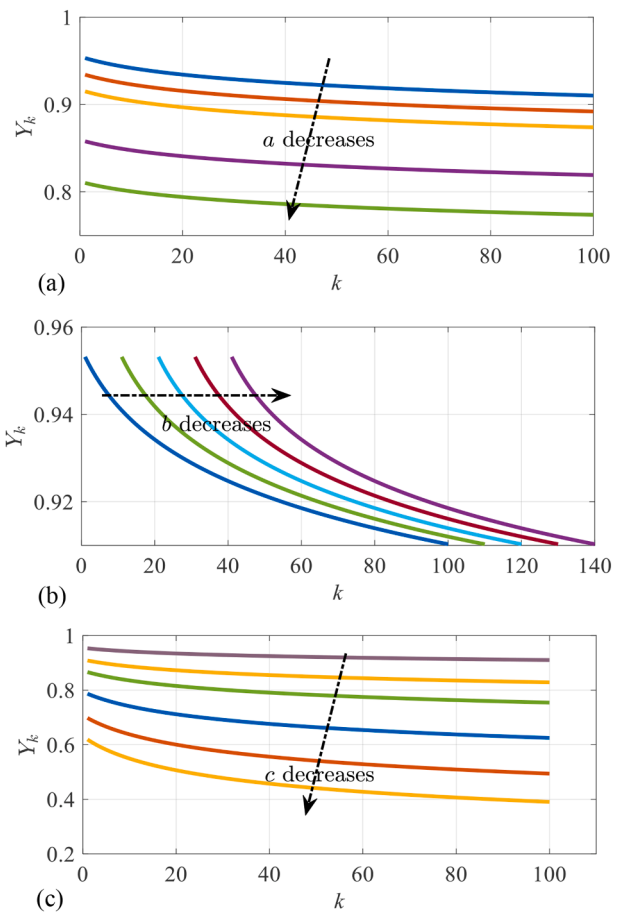

Fig. 2. Influence of each parameter change on the power model. (a) Parameter a changed and parameters b and c fixed. (b) Parameter b changed and parameters a and c fixed. (c) Parameter c changed and parameters a and b fixed.

Table 1
Quantitative indices of fitting results for real data in Fig. 1.

Data	Fit type	SSE	R-square	Adj. R-square	RMSE
Real data 1	$Y_k = a_0(k+d_0)^{c_0}$	0.0012	0.9997	0.9997	0.0013
	$Y_k = a_0(k+d_0)^{c_0} + b_0$	0.0012	0.9997	0.9997	0.0012
Real data 2	$Y_k = a_0(k+d_0)^{c_0}$	0.0030	0.9999	0.9999	0.0011
	$Y_k = a_0(k+d_0)^{c_0} + b_0$	0.0030	0.9999	0.9999	0.0011

Table 2
Selected degradation models for performance comparison.

Models	Explanation	Mathematical Expression
Model 1	CE model	$Y_k = ab^k + c$
Model 2	Square-root-of-time model	$Y_k = ak^{1/2} + b$
Model 3	Two-term logarithmic model	$Y_k = a + b\log(k+1) + c\log(1-k/(d+2))$
Model 4	Two-term exponential model	$Y_k = ae^{bk} + ce^{dk}$
Model 5	Quadratic polynomial model	$Y_k = ak^2 + bk + c$
Model 6	One-term exponential model	$Y_k = ae^{bk}$

Eq. (5) uses parameter c to adjust the shape of capacity degradation. When the shape parameter c equals 0.5, the proposed model can be seen as a similar generalized model to the traditional square-root-of-time model. On the other hand, when parameter c equals a different number, the proposed model can fit different types of degradation curves. For example, in Fig. 1, when $c < -1$, it is a monotonically decreasing convex curve. When $-1 < c < 0$, it denotes a monotonically decreasing concave curve. With the change of parameter c, the capacity degradation rate is significantly different.

Parameter b is a constant term, which can adjust for the cycle number with an unknown initial cycling value. For instance, the fitting result of a battery that has been used for many cycles is consistent with the result of the same battery with the initial cycle. In addition, parameter a depicts the linear relationship of capacity with cycle number.

Thus, the proposed model has good potential to fit different types of degradation paths. For example, Lin et al. [30] utilized the power model to depict the scale parameter of the gamma process. The proposed Gamma process model can better fit the degradation data than the compared one-phase gamma process model in terms of the Akaike information criterion, and the proposed model accurately predicts the degradation behavior of four battery cells. Thus, the proposed model can be regarded as taking into account more information than the traditional model.

The influence of each parameter change on the power model is discussed in Fig. 2. In Fig. 2(a), we fix the parameter b and c, and then change parameter a. It can be seen that the scale of the curve is stretched or compressed in the direction of the Y-axis. Thus, parameter a is called the scale parameter. The next Fig. 2(b) denotes the condition with parameters a and c fixed, and parameter b changed. The curve translates along the x-axis, which is equivalent to adding or decrease the cycle. Thus, parameter b is named as the location parameter. Finally, in Fig. 2 (c), as parameter c changes when parameters a and b are fixed, we can see the curvature increases or decreases, and then the curve shape changes correspondingly. Thus parameter c is named as the shape parameter.

2.2. Other existing degradation models

To verify the performance of proposed model on degradation modeling and RUL prediction, a total of six existing representative models listed in Table 2 are chosen for comparison in this work. In short, the square-root-of-time model [27] and CE model [12] are both typical semi-empirical models. To validate the modeling performance of power model sufficiently, four empirical models including two-term logarithmic model [22], one-term exponential model [21], two-term exponential model [18], and quadratic polynomial model [19], are selected. The comparative results on model fitting and RUL prediction will be presented on Section 4. In this section, we give a brief review on selected five other models.

(1) Coulombic efficiency-based model

The CE model was a semi-empirical model derived from the relationship between columbic efficiency and degradation rate [12]:

$$Y_k = ab^k + c, \tag{6}$$

where a, b, c are model unknown parameters and b indicates the CE of lithium-ion battery; k is the cycle time and Y_k denotes the maximum available capacity in cycle k. In this paper, we use this model as a comparison method because the CE model was reported to effectively capture the convex degradation trend of lithium-ion batteries.

(2) Two-term logarithmic model

The two-term logarithmic model was first put forward by Yang et al. [22]. This model can effectively depict the degradation path with two-phase behaviors, which includes a fast degradation phase and a slow degradation phase. The model is formulated as:

$$Y_k = a + b\log(k+1) + c\log(1-k/(d+2)), \tag{7}$$

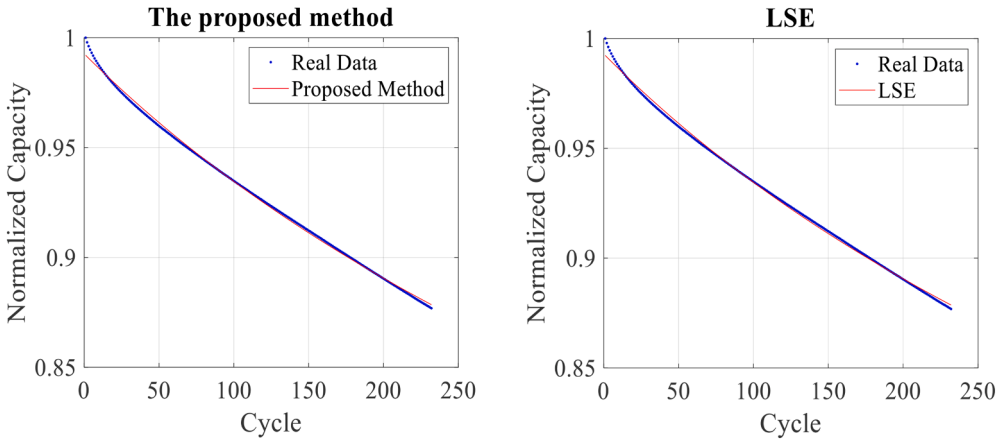

(a): Computing time of parameter estimation: 0.038s
R-square: 0.9984

(b): Computing time of parameter estimation: 0.501s
R-square: 0.9984

Fig. 3. Parameter estimation and fitting results obtained by (a) the proposed method and (b) LSE.

where a, b, c, and d are unknown parameters of the model.

(3) **One-term exponential model**

The exponential function is a traditional empirical model, which models the increase of internal impedance caused by SEI thickening with the iterations growing. Since battery degradation fade is closely related to the internal impedance, one term exponential model is an effective model to depict the degradation path [21,33]. This model is expressed as:

$$Y_k = ae^{bk}, \tag{8}$$

where a and b are unknown parameters.

(4) **Two-term exponential model**

Regression results of several experimental data indicate that another exponential model can depict the battery degradation fade more accurately. This model, named a two-term exponential model, is denoted as [18,32,34]

$$Y_k = ae^{bk} + ce^{dk}, \tag{9}$$

where a, b, c, and d are unknown parameters of the model.

(5) **Quadratic polynomial model**

Micea et al. first used the quadratic polynomial model as an empirical model to fit the data between the stored maximum capacity function Y_k and charge/discharge cycle k [19]. This model is given by

$$Y_k = ak^2 + bk + c, \tag{10}$$

where a, b, and c are unknown parameters of the model.

3. Battery remaining useful life prediction

In this section, a two-phase prediction method including a statistical inference and a Bayesian filter is developed for battery RUL prediction based on the proposed model. The statistical inference is aimed to obtain the point estimators of the parameters based on the observed data. Then the point estimators are served as the initial value of Bayesian filter to conduct online RUL prediction.

3.1. Statistical inference and offline parameter estimation

The statistical inference of the proposed model is given in this section. To transform the complex nonlinear relationship into a linear relationship, first, take logarithms on both sides of the model Eq. (5),

$$\ln Y_k = \ln(a(k+b)^c) = c\ln(k+b) + \ln a. \tag{11}$$

Note that $\ln Y_k$ has a linear relationship with $\ln(k+b)$. Thus, calculate their Pearson's correlation coefficient.

$$r(\ln Y_k, \ln(k+b)) = \frac{\mathrm{Cov}(\ln Y_k, \ln(k+b))}{\sqrt{\mathrm{Var}(\ln Y_k) * \mathrm{Var}(\ln(k+b))}}. \tag{12}$$

However, because of the existence of noise, the Pearson's correlation coefficient is less than 1. To eliminate the interference of the noise, we maximize the absolute value of the Pearson's correlation coefficient to make the model better fit the degradation capacity. Thus, the estimator of b can be denoted as

$$\widehat{b} = \underset{b}{\mathrm{argmax}} \frac{|\mathrm{Cov}(\ln Y_k, \ln(k+b))|}{\sqrt{\mathrm{Var}(\ln Y_k) * \mathrm{Var}(k+b)}}. \tag{13}$$

Next, the substitute estimator $\widehat{b}$ into Eq. (11), we can get

$$\ln Y_k = c\ln(k+\widehat{b}) + \ln a. \tag{14}$$

See $\ln(k+\widehat{b})$ as an independent variable, and $\ln Y_k$ as a dependent variable. From the Eq. (14), the independent variable and dependent variable have a linear relationship. Thus, according to Gaussian-Markov Theorem (For example, see Rao [35]), conduct linear regression between independent variable $\ln(k+\widehat{b})$ and dependent variable $\ln Y_k$, we can get

$$\begin{cases} \widehat{c} = \dfrac{\sum_{i=1}^{n}(\ln(k_i+\widehat{b}) - \overline{\ln(k+\widehat{b})})(\ln Y_{k_i} - \overline{\ln Y_k})}{\sum_{i=1}^{n}(\ln(k_i+\widehat{b}) - \overline{\ln(k+\widehat{b})})^2}, \\ \widehat{\ln a} = \overline{\ln Y_k} - \widehat{c}\,\overline{\ln(k+\widehat{b})}. \end{cases} \tag{15}$$

Further, after simple transformation,

$$\widehat{a} = e^{\overline{\ln Y_k} - \widehat{c}\,\overline{\ln(k+\widehat{b})}}. \tag{16}$$

Thus, we finish deriving the expressions of point estimators $\widehat{a}$, $\widehat{b}$, $\widehat{c}$.

The proposed estimation method can be compared with the commonly used least square estimation (LSE). In fact, from the perspective of computation efficiency, the proposed method has lower computation time than LSE, this is because except for a single variable

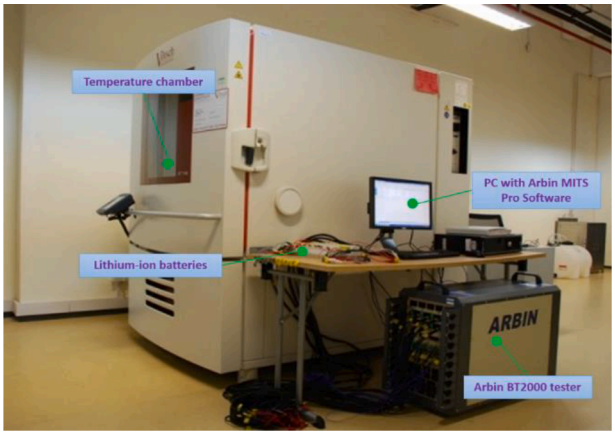

Fig. 4. Experimental condition.

Table 3
Battery parameters.

Battery Type: BAK 18,650 LFP battery	
Anode	Graphite
Nominal Voltage	3.2V
Nominal Capacity	1 Ah
Upper/Lower Cutoff Voltage	3.6 V/2V
End of Charge Current	0.05C
Maximum Continuous Discharge Current	30A

optimization, other procedures can be expressed as an analytic mathematical expression in the proposed method. However, the LSE needs a three-variable optimization, this greatly improves the computation complexity. To verify the estimation efficiency and accuracy for the proposed estimation method and LSE, we also conduct an experiment as follows:

We adopt 232 cycle data to verify the effectiveness of the proposed model. For fitting accuracy, the results are shown in the following Fig. 3:

In the same computing environment, for LSE, the R-square equals 0.9984 and the computing time is 0.501s; for the proposed method, the R-square equals 0.9984, and the computing time is 0.038s. From the two results, we can see that the fitting results are almost the same, but the consumed time of the proposed method is much less than LSE. Computing time is an important index for the real-time online prediction method. Thus, the proposed method is recommended.

3.2. Online RUL prediction based on particle filter

To employ the proposed model for online RUL prediction in real-lifetime applications, the following issues must be considered: 1) When using a new batch of cells, there is little information on the model parameters. 2) Because there exists a difference between cell to cell, it is not suitable to apply the fitted parameters in the laboratory directly to the EV. 3) Environmental noise, measurement error of sensors, and operational factors lead to uncertainties, which render the proposed model inaccurate. 4) Real-time response needs a great demand for computing speed, and this makes the offline parameter estimation inapplicable. To address these issues, a Bayesian filtering framework is proposed incorporating the proposed model for online battery RUL prediction. The specific procedure of the framework includes model construction, state estimation based on Bayesian filter, and posterior distribution calculation using PF.

(1) **Model construction**

First assume the state transformation process of battery capacity subject to the first-order Markov process, which follows two basic properties 1) State parameter at the current cycle only depends on the state at the last cycle x_k. 2) Observed capabilities C_k are independent of each other, and only determined by the state x_k at cycle k. Based on these two properties, we construct the state-space function. The parameter vector $x_k = [a_k, b_k, c_k]^T$ is chosen as the system state at cycle k. According to the Markov assumption of the system model, the k state of the system only depends on its last state k-1, and we assume the process from k-1 to k is subject to a zero-mean Gaussian random walk. Thus, the systems state function can be denoted as

$$\mathrm{x_k} = \mathrm{x_{k-1}} + \varepsilon = \begin{bmatrix} a_k \\ b_k \\ c_k \end{bmatrix} = \begin{bmatrix} a_{k-1} \\ b_{k-1} \\ c_{k-1} \end{bmatrix} + \begin{bmatrix} \varepsilon_0 \\ \varepsilon_1 \\ \varepsilon_2 \end{bmatrix}, \begin{bmatrix} \varepsilon_0 \sim N(0, \sigma_0^2) \\ \varepsilon_1 \sim N(0, \sigma_1^2) \\ \varepsilon_2 \sim N(0, \sigma_2^2) \end{bmatrix}, \tag{17}$$

where $\varepsilon = (\varepsilon_0, \varepsilon_1, \varepsilon_2)$ denotes the additive Gaussian noise with a standard deviation $(\sigma_0, \sigma_1, \sigma_2)$. In fact, the battery capacity only depends on the state function in Eq. (17), and their relationship can be depicted using the model proposed in Section 2. However, when measuring the battery capacity, there exist uncertainties caused by sensors measurement, manual operation, environmental factors and so on. Thus, an additive Gaussian noise v is also assumed to refer to the measurement uncertainty. Then, the measurement function can be denoted as

$$Y_k = h(x_k) + v = a_k(k + b_k)^{c_k} + v\ , v \sim N(0, \sigma_v^2), \tag{18}$$

where σ_v denotes the standard deviation of the Gaussian noise v. Here we assumed measurement Y_k is noisy, that's to say there exist some measurement errors caused by the sensors. In this framework, the model parameters are chosen as states, which are unobserved and will change with battery degradation. The measurement Y_k is the capacity of the battery. In the experiment, the battery capacity can be measured at every cycle. Then the predicted Y_k (prior information) and the measured Y_k (the likelihood information) are used to estimate the updated state parameters (posterior information). Finally, the updated state parameters (posterior information) are used to make further predictions.

(2) **State estimation based on Bayesian filter**

The Bayesian filter, which is implemented to estimate the system state x_k, can be divided into two steps: Prediction and update. Specifically, first, predict the distribution of the hidden state function x_k based on (k-1)th observation Y_{k-1}. Next, update the distribution of the hidden state function utilizing prediction and kth observation Y_k. These two steps can be expressed as follows:

Prediction:

$$p(x_k|Y_{1:k-1}) = \int p(x_k|x_{k-1})p(x_{k-1}|Y_{1:k-1})dx_{k-1}. \tag{19}$$

Update:

$$p(x_k|Y_{1:k}) = \frac{p(Y_k|x_k)p(x_k|Y_{1:k-1})}{\int p(Y_k|x_k)p(x_k|Y_{1:k-1})dx_k}. \tag{20}$$

(3) **Posterior distribution calculation using PF**

However, when the Bayesian filter is implemented to estimate the state, a common problem often occurs that the posterior distribution is too complicated to analyze. Thus, the PF, as a Sequential Importance Monte Carlo Sampling method, is an effective method to overcome this problem. PF essentially solves this problem by looking for a group of random samples propagating in the state space to approximate the probability density function (PDF), then using these samples to substitute the integral operation, and finally obtaining the minimum variance estimation of the system state function. These processes can be

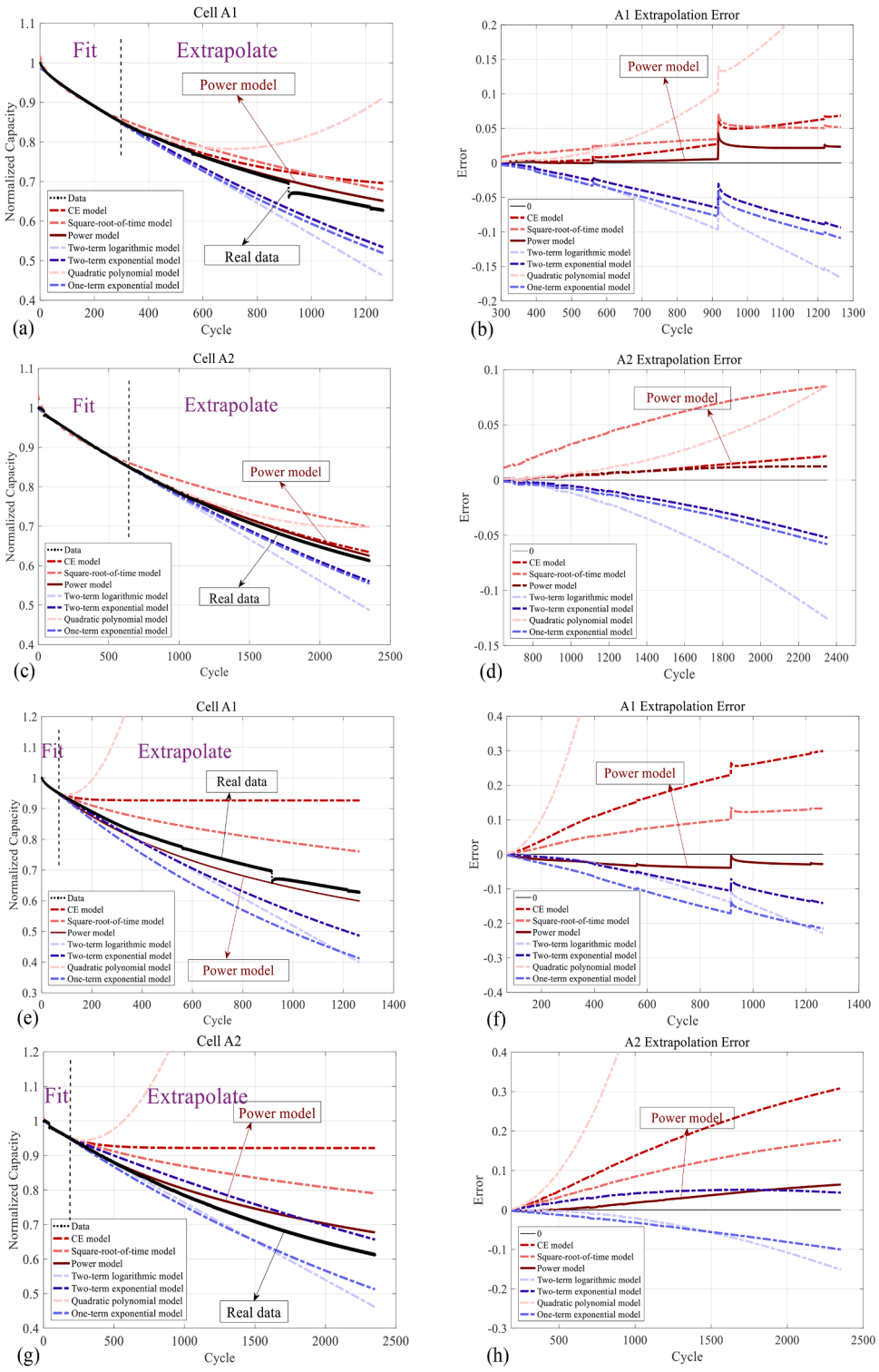

Fig. 5. Fitting and extrapolation results. 1) 15% for fitting and 85% for extrapolation: (a-b) cell A1; (c-d) cell A2. 2) 5% for fitting and 95% for extrapolation: (e-f) cell A1; (g-h) cell A2.

expressed in Eqs. (21) and (22).

$$p(\mathrm{x_k}|Y_{1:k}) \approx \sum_{i=1}^{N_s} \widetilde{\omega}_k^{i_p} \delta\left(\mathrm{x_k} - \mathrm{x_k^{i_p}}\right), \tag{21}$$

$$\widetilde{\omega}_k^{i_p} = \frac{\omega_k^{i_p}}{\sum_{i=1}^{N_s} \omega_k^{i_p}}, \tag{22}$$

where $\delta(\cdot)$ denotes the Dirac delta function and $\widetilde{\omega}_k^{i_p}$ denotes the normalized weight. Next, the system state function can be approximated as

$$\mathrm{x_k} = \int_{-\infty}^{+\infty} \mathrm{x_k} p(\mathrm{x_k}|Y_{1:k}) dx_k = \sum_{i=1}^{N_s} \widetilde{\omega}_k^{i_p} \mathrm{x_k^{i_p}}. \tag{23}$$

Table 4
Quantitative extrapolation accuracy in Fig. 5.

Figure	Model	MSE	RMSE	MAE
Fig. 5(a) and (b)	CE model	0.00128	0.03575	0.02710
	Square-root-of-time model	0.00139	0.03726	0.03399
	Power model	**0.00020**	**0.01424**	**0.00991**
	Two-term logarithmic model	0.00724	0.08508	0.07068
	Two-term exponential model	0.00272	0.05213	0.04504
	Quadratic polynomial model	0.01600	0.12648	0.09282
	One-term exponential model	0.00391	0.06255	0.05493
Fig. 5(c) and (d)	CE model	0.00014	0.01196	0.01012
	Square-root-of-time model	0.00344	0.05865	0.05435
	Power model	**0.00008**	**0.00892**	**0.00811**
	Two-term logarithmic model	0.00377	0.06137	0.04900
	Two-term exponential model	0.00069	0.02631	0.02133
	Quadratic polynomial model	0.00148	0.03844	0.02938
	One-term exponential model	0.00092	0.03029	0.02521
Fig. 5(e) and (f)	CE model	0.03688	0.19203	0.17026
	Square-root-of-time model	0.00769	0.08770	0.07817
	Power model	**0.00077**	**0.02777**	**0.02630**
	Two-term logarithmic model	0.01234	0.11108	0.08722
	Two-term exponential model	0.00619	0.07866	0.06580
	Quadratic polynomial model	10.0181	3.16514	2.36965
	One-term exponential model	0.01718	0.13107	0.11489
Fig. 5(g) and (h)	CE model	0.03725	0.19301	0.16920
	Square-root-of-time model	0.01303	0.11416	0.10129
	Power model	**0.00130**	**0.03602**	**0.02913**
	Two-term logarithmic model	0.00471	0.06864	0.05123
	Two-term exponential model	0.00172	0.04152	0.03904
	Quadratic polynomial model	2.32616	1.52518	1.15347
	One-term exponential model	0.00301	0.05488	0.04671

The weight of each particle is updated as follows,

$$\widetilde{\omega}_k^{i_p} \propto \widetilde{\omega}_{k-1}^{i_p} \frac{p\left(Y_k|\mathrm{x}_\mathrm{k}^{\mathrm{i_p}}\right)p\left(\mathrm{x}_\mathrm{k}^{\mathrm{i_p}}|\mathrm{x}_{\mathrm{k-1}}^{\mathrm{i_p}}\right)}{\pi\left(\mathrm{x}_\mathrm{k}^{\mathrm{i_p}}|\mathrm{x}_{\mathrm{0:k-1}}^{\mathrm{i_p}}, Y_{1:k}\right)}, \tag{24}$$

where $\pi(x_k^{i_p}|x_{0:k-1}^{i_p}, Y_{1:k}) = \pi(x_k^{i_p}|x_{0:k-1}^{i_p}, Y_k)$ denotes the importance distribution. A most popular choice of the importance distribution is a prior distribution $\pi(x_k^{i_p}|x_{0:k-1}^{i_p}, Y_k) = p(x_k^{i_p}|x_{k-1}^{i_p})$. Here based on the PF method, similar to Ref. [12], the Probability Density Function (PDF) of RUL at the current cycle number M can be calculated through the following equation:

$$\mathrm{RUL}(x) = \frac{1}{N_p}\sum_{i_p=1}^{N_p}\delta\left(M + x - \underset{k}{\mathrm{argmin}}\left(a_M^{i_p}\cdot\left(b_M^{i_p}+k\right)^{c_M^{i_p}} < 0.8\right)\right), \tag{25}$$

where random variable x denotes the remaining useful lifetime. Given the PDF in Eq. (25), the RUL confidence interval and point estimation can both be estimated.

In conclusion, the process of PF-based RUL prediction can be generally divided into five steps: Initialization, Prediction, Update, Resampling and Estimating.

Step 1: Initialization($k = 0$)

First, draw N_p particles from prior distribution $\pi(x_0)$. Then equally assign the weight $\omega_0^{i_p}$ of these N_p particles, $\omega_0^{i_p} = 1/N_p$, $i_p = 1,2,\ldots, N_p$.

Step 2: Prediction($k = 1,2,3,\ldots$)

Using state function (17) to propagate particles from distribution $\pi(x_k|x_{k-1}^{i_p})$, $i_p = 1,2,\ldots,N_p$.

Step 3: Update($k = 1,2,3,\ldots$)

First update the weights of each particle based on Eq. (24), and then normalize the updated weights using Eq. (22). Finally use Eq. (23) to estimate the system states.

Step 4: Resampling($k = 1,2,3,\ldots$)

Step 4 is devoted to verifying whether the effective particle number N_E falls below the threshold N_T. An estimator based on rule of thumb is given by[36]

$$\widehat{N}_E = \frac{1}{\sum_{j=1}^{N_p}\left(\omega_k^j\right)^2}. \tag{26}$$

Then conduct the resampling process when $\widehat{N}_E < N_T$.

Step 5: Estimating

Estimate RUL of the battery using PDF (25).

4. Experimental results

This Section focuses on the experimental verification of the proposed power model. First, Section 4.1 illustrates the specific experimental procedure and data acquisition. Then, the model fitting and extrapolation results are discussed in Section 4.2. Finally, Section 4.3 concentrates on verifying the RUL prediction results based on the power model.

4.1. Experimental data

The experimental setup, as shown in Fig. 4, is same as in [12,37]. The setup includes a Votsch temperature chamber to control the ambient temperature of the batteries and an Arbin BT2000 battery test system to load and sample the lithium-ion batteries. To control the whole experiment and log the test data, a computer equipped with Arbin's Mits Pro-software is used. The experimental data are then processed and analyzed using a PC.

Four lithium iron phosphate (LFP) batteries with 18,650 type were tested in this experiment, and their basic parameters are tabulated in Table 3. The procedure involved a constant current charge-discharge life cycle test, with each cycle comprising of a 1C charge process under constant current and constant voltage mode, followed by a 1C discharge process. The cut-off voltages for the charge and discharge processes were 3.6 V and 2 V, respectively, while the end of charge current for the charge process was 0.05C. In other words, the batteries were fully charged and discharged in each cycle, with the depth of charge and discharge both equal to 100%. To reduce experiment time and environmental noise effects, the temperature stress was increased to 45℃. The accelerated experiment lasts until the capacity drops below 80% of the nominal capacity, which is same as the battery failure threshold [12]. The maximum remaining capacity is then calculated using the standard Coulomb counting method [38], and the collected capacity is used to verify the proposed model and RUL prediction method. Throughout the whole paper, normalized capacity, which is defined as

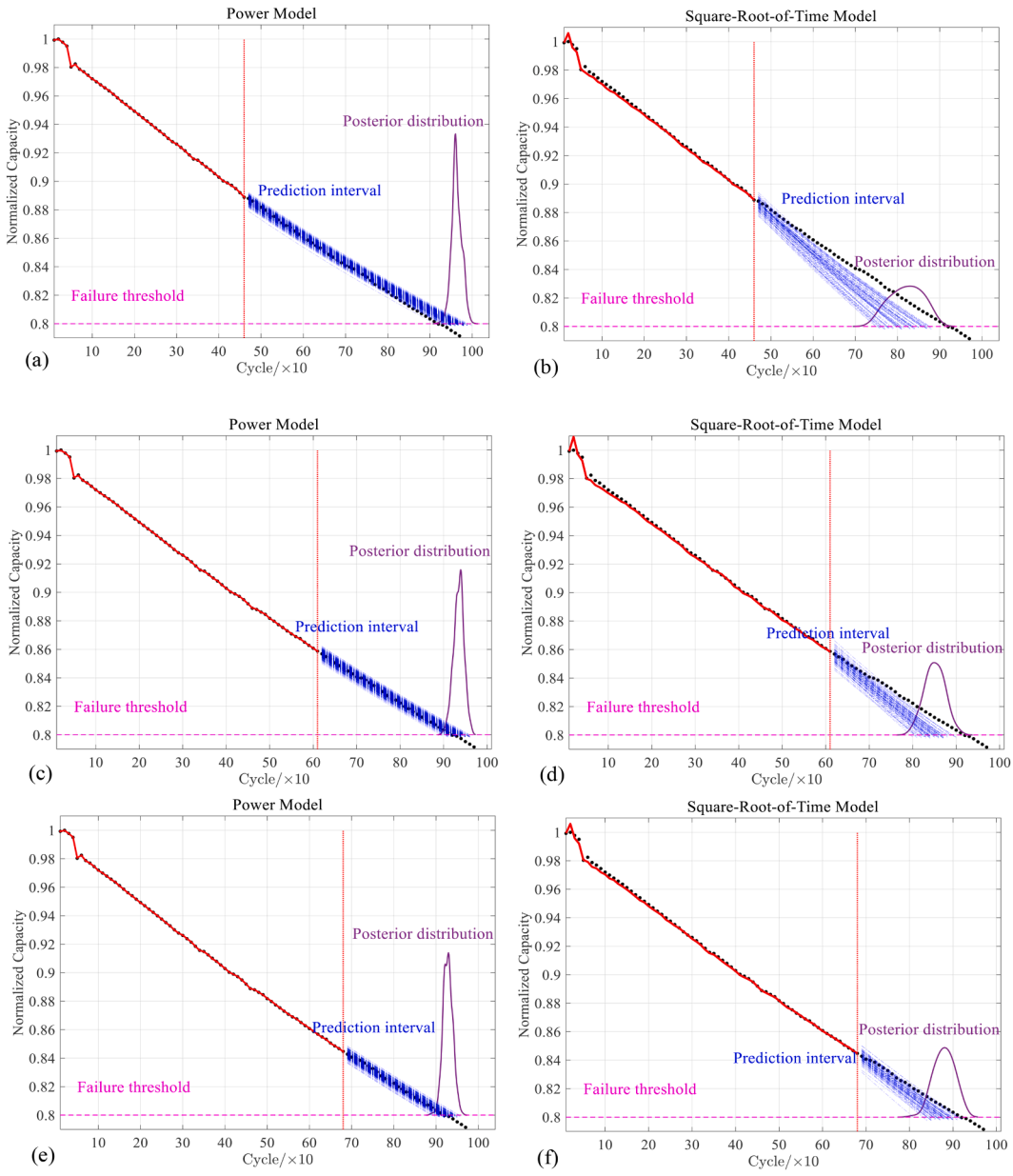

Fig. 6. Online RUL predictions by the power model (left) and the square-root-of-time model (right): (a-b) predictions from the first 1/2 of the lifetime; (c-d) predictions from the first 2/3 of the lifetime; (e-f) predictions from the first 3/4 of the lifetime.

Table 5
RUL prediction accuracy of Fig. 6.

Prediction Rotation	True RUL	Model	Absolute Error	Relative Error
1/2 of lifetime	46	Power model	4.33	9.4%
		Square-root-of-time model	9.92	21.6%
2/3 of lifetime	31	Power model	1.47	4.7%
		Square-root-of-time model	6.94	22.4%
3/4 of lifetime	24	Power model	0.80	3.3%
		Square-root-of-time model	4.02	16.8%

the ratio of the maximum remaining capacity in initial status to the nominal capacity, is used to indicate the battery state of health.

4.2. Results of modeling

To analyze the model precision based on the model-evaluation data, the first 5% and 15% data is used for fitting. Fig. 5 plots the fitting curve and predicting curve with the real degradation path, with a comparison of other models listed in Table 2. Obviously, the closer the model curve is to the real data, the fitting and prediction effect of the model will be, and their quantitative results are listed in Table 4. Two battery cells are used here for testing, while others are used for training. In Fig. 5(a) and (c), the first 15% data are used for fitting and the last 85% data is used for extrapolation, and their corresponding extrapolation errors are shown in Fig. 5(b) and (d). Besides, in Fig. 5(e) and (g), the first 5% data are used for fitting and the last 95% data are used for extrapolation, and the corresponding extrapolation errors are shown in Fig. 5(f) and (h). In Fig. 5(a), (c), (e), and (g), results show that compared with extrapolation

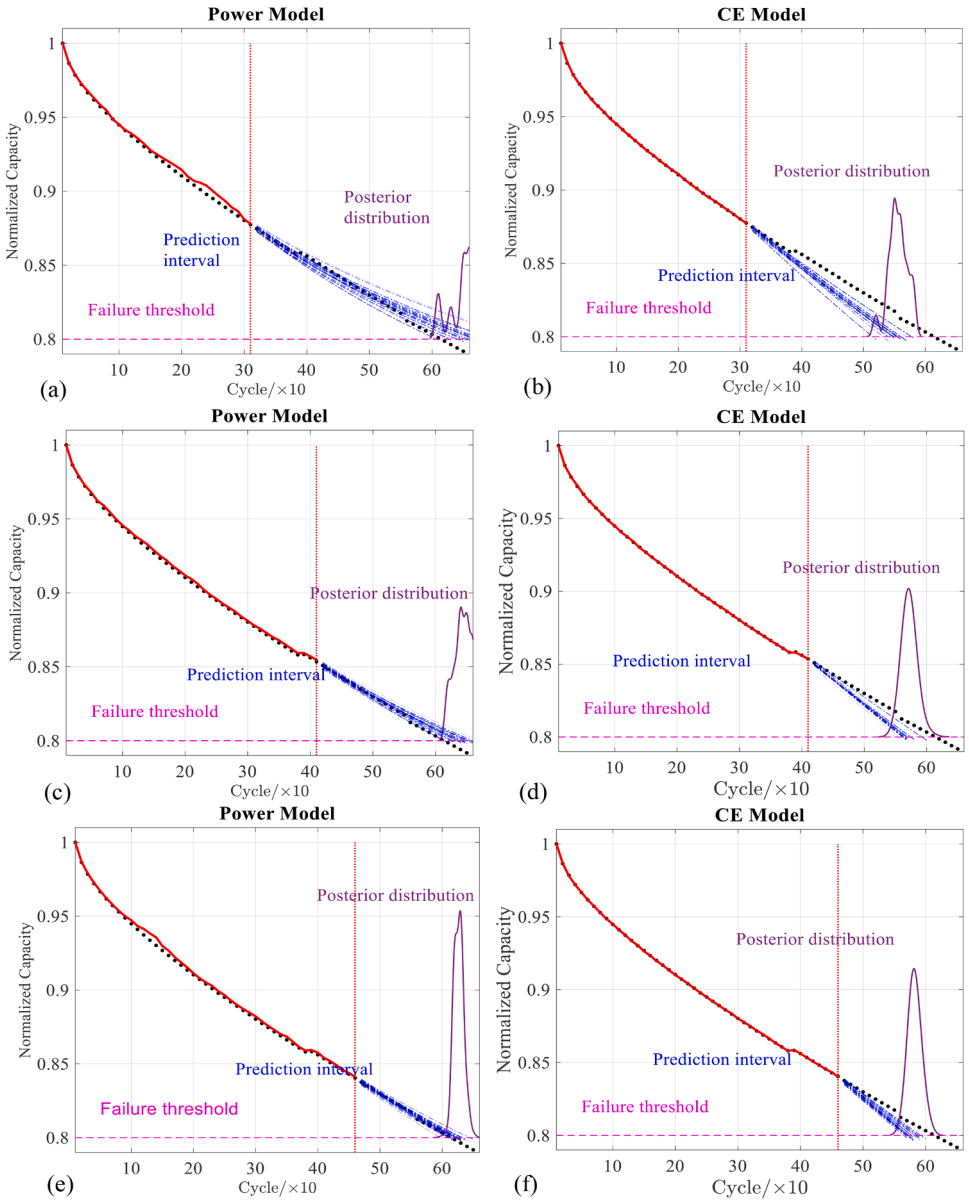

Fig. 7. Online RUL predictions by the power model (left) and the CE model (right): (a-b) predictions from the first 1/2 of the lifetime; (c-d) predictions from the first 2/3 of the lifetime; (e-f) predictions from the first 3/4 of the lifetime.

Table 6
RUL prediction accuracy of Fig. 7.

Prediction Rotation	True RUL	Model	Absolute Error	Relative Error
1/2 of lifetime	31	Power model	4.12	13.3%
		Columbic model	6.41	20.7%
2/3 of lifetime	21	Power model	2.30	11.0%
		Columbic model	4.78	22.8%
3/4 of lifetime	16	Power model	0.66	4.1%
		Columbic model	3.75	23.4%

deviation, the fitting deviation is so small that can be generally ignored. Thus, the quantitative extrapolation deviation is mainly discussed in Table 4, and we analyze the extrapolation results in Fig. 5 in detail.

In Fig. 5(a) and (e), it is obvious that the extrapolation accuracy of the power model is the highest among these methods. The corresponding quantitative results in Table 4 also supports that result: the MSE, RMSE and MAE of the power model are the smallest. In Fig. 5 (c), at the beginning of extrapolation (almost from 800 to 1500 cycles), the power model and CE model are very close, but in the second half (1500–2200), the power model shows great advantages to other models. Besides, according to quantitative results in Line 11 of Table 4, the MSE of the power model equaling 0.0008 is also the smallest among the comparison models. In Fig. 5(g) and (h), in the main part (almost from 200 to 1800 cycles), the power model performs the best among the comparison 6 methods. But at the end of the cycle (almost from 1800 to 2300), the two-term exponential model slightly exceeds the power model. However, the corresponding capacity of this part is lower than 0.75. As mentioned, in practical problems, capacity lower than 80% of the nominal level usually means the battery has reached its lifetime. Thus, the end of the cycle (1800–2300) corresponding to nominal capacity level lower than 0.75 has limited practical value for RUL prediction. Besides, from the quantitative indices in Table 4, the MSE 0.0013 of the proposed power model is also the smallest among these 7 models, thus, the power model generally performs best in Fig. 5(g).

In conclusion, results in Fig. 5 and Table 4 show that among all the models, the power model has the smallest MSE, RMSE, and MAE. Compared with traditional square-root-of-time model, its extrapolation prediction accuracy has been greatly improved. Thus, from the perspective of fitting and extrapolation, the power model is recommended.

4.3. Results of RUL prediction

After verifying the fitting and extrapolation property model, in this section, the online RUL prediction based on the power model is conducted, compared with that based on the square-root-of-time model and the CE model. For ease of understanding and presentation, the capacity data are sampled every 10 cycles.

Fig. 6 shows the RUL prediction of Cell A2 based on the power model and the square-root-of-time model, with predictions made at the 1/2, 2/3, 3/4 lifetime points, respectively. Table 5 tabulates the quantitative indices of Fig. 6. In each prediction, the prediction interval of the power model (on the left) is not only narrower, but also has more covering rate to the real degradation path than the compared square-root-of-time model (on the right). This indicates the RUL prediction accuracy based on the proposed power model is significantly higher than that based on the square-root-of-time model. The quantitative indices in Table 5 also support the above-mentioned conclusion: the relative errors of proposed model in all cases are significantly lower than those of the square-root-of-time model.

As in Ref. [12], Yang et al. proposed a semi-empirical CE model, and verified the CE model outperformed the traditional square-root-of-time model in terms of online RUL prediction. In this section, we also add a new dataset to compare the prediction performance of proposed model with the CE model. Fig. 7 and Table 6 show the RUL prediction results based on Cell A3.

Results show the proposed power outperforms the CE model in terms of prediction accuracy on the new dataset. To sum up, RUL prediction based on the power model has better prediction accuracy, thus is recommended.

5. Conclusion

Motivated by two concerns of the widely-used square-root-of-time model, this paper proposes a new power model to depict the degradation path of LFP batteries. The proposed power model is obtained by three-step transformation of the traditional square-root-of-time model, where the three steps include model extension of power exponent, model extension of cycle number and model simplification. Then several representative properties of the power model are investigated for applications. For online RUL prediction based on the proposed model, an RUL prediction method, including an offline parameter estimation algorithm and a PF algorithm, is proposed. The output point estimators of the offline algorithm are substituted as the initial value of the PF algorithm for further online RUL prediction.

The LFP battery degradation experiment is conducted to verify the effectiveness of the power model and the RUL prediction algorithm. First, based on the experiment data, the fitting and extrapolation accuracy of the proposed power model is verified. Fitting results show that the power model almost performs as well as the six representative comparison models, but extrapolation results indicate the power model has smaller predicting errors measured by MSE, RMSE and MAE than those competing models. Second, the experiment data are also used to verify the online RUL prediction properties of the power model. Results indicate that the online prediction accuracy based on the power model outperforms the square-root-of-time model and the CE model. Thus, the RUL prediction method based on the power model is recommended.

In the future, other factors, such as temperature, depth-of-charge, and depth-of-discharge, are also worth studying. The quantified relationships between these factors and the power model can also be constructed, and these relationships can be modelled and further used for RUL prediction in practice.

CRediT authorship contribution statement

Fanbing Meng: Writing – original draft, Software, Methodology, Investigation, Conceptualization. **Fangfang Yang:** Writing – review & editing, Software, Data curation. **Jun Yang:** Writing – review & editing, Methodology. **Min Xie:** Writing – review & editing.

Declaration of Competing Interest

The authors declare that they have no known competing financial interests or personal relationships that could have appeared to influence the work reported in this paper.

Data availability

The data that has been used is confidential.

Acknowledgements

This research acknowledges the support provided by National Natural Science Foundation of China (62203482, 71971181), by Guangdong Basic and Applied Basic Research Foundation (2021A1515110354), by Research Grant Council of Hong Kong (11200621), and also by Hong Kong Innovation and Technology Commission (InnoHK Project CIMDA).

References

[1] Zhang Y, Xiong R, He H, Shen W. Lithium-ion battery pack state of charge and state of energy estimation algorithms using a hardware-in-the-loop validation. IEEE Trans Power Electron 2016;32:4421–31.
[2] Severson KA, Attia PM, Jin N, Perkins N, Jiang B, Yang Z, et al. Data-driven prediction of battery cycle life before capacity degradation. Nature Energy 2019;4:383–91.
[3] Hu X, Xu L, Lin X, Pecht M. Battery lifetime prognostics. Joule 2020;4(2):310–46.
[4] Zhu R, Chen Y, Peng W, Ye Z-S. Bayesian deep-learning for RUL prediction: an active learning perspective. Reliab Eng Syst Saf 2022;228:108758.
[5] Tang T, Yuan H. A hybrid approach based on decomposition algorithm and neural network for remaining useful life prediction of lithium-ion battery. Reliab Eng Syst Saf 2022;217:108082.
[6] Laayouj N, Hicham J. Lithium-ion battery degradation assessment and remaining useful life estimation in hybrid electric vehicle. Renewable Energy Sustainable Development 2016;2(1):37–44.
[7] Wang Y, Rui P, Yang D, Tang X, Chen Z. Remaining useful life prediction of Lithium-ion battery based on discrete wavelet transform. Energy Procedia 2017;105:2053–8.
[8] Mcculloch WS, Pitts W. A logical calculus of the ideas immanent in nervous activity. Bull Math Biophys 1943;5:115–33.
[9] Ardeshiri RR, Liu M, Ma C. Multivariate stacked bidirectional long short term memory for lithium-ion battery health management. Reliab Eng Syst Saf 2022;224:108481.
[10] Xu F, Yang F, Fei Z, Huang Z, Tsui K-L. Life prediction of lithium-ion batteries based on stacked denoising autoencoders. Reliab Eng Syst Saf 2021;208:107396.
[11] Gordon NJ, Salmond DJ, Smith AF. Novel approach to nonlinear/non-Gaussian Bayesian state estimation. In: IEE Proceedings F-radar and signal processing. IET; 1993. p. 107–13.
[12] Yang F, Song X, Dong G, Tsui KL. A coulombic efficiency-based model for prognostics and health estimation of lithium-ion batteries. Energy 2019;171:1173–82.
[13] Darling R, Newman J. Modeling side reactions in composite LiyMn2O4 electrodes. J Electrochem Soc 1998;145:990.
[14] Dai Y, Cai L, White RE. Capacity fade model for spinel LiMn2O4 electrode. J Electrochem Soc 2012;160:A182.
[15] Xu X, Tang S, Yu C, Xie J, Han X, Ouyang M. Remaining useful life prediction of lithium-ion batteries based on wiener process under time-varying temperature condition. Reliab Eng Syst Saf 2021;214:107675.
[16] Gao Y, Zhu C, Zhang X. Global parameter sensitivity analysis of electrochemical model for Lithium-ion batteries considering aging. IEEE/ASME Trans Mechatron 2021;26(3):1283–94.
[17] Ramadesigan V, Northrop PW, De S, Santhanagopalan S, Braatz RD, Subramanian VR. Modeling and simulation of lithium-ion batteries from a systems engineering perspective. J Electrochem Soc 2012;159:R31.

[18] He W, Williard N, Osterman M, Pecht M. Prognostics of lithium-ion batteries based on Dempster–Shafer theory and the Bayesian Monte Carlo method. J Power Sources 2011;196:10314–21.
[19] Micea MV, Ungurean L, Carstoiu GN, Groza V. Online state-of-health assessment for battery management systems. IEEE Transa Instrumentat Measurement 2011;60:1997–2006.
[20] Xing Y, Ma EW, Tsui K-L, Pecht M. An ensemble model for predicting the remaining useful performance of lithium-ion batteries. Microelectron Reliab 2013;53:811–20.
[21] Wang D, Yang F, Tsui K-L, Zhou Q, Bae SJ. Remaining useful life prediction of lithium-ion batteries based on spherical cubature particle filter. IEEE Trans Instrum Meas 2016;65:1282–91.
[22] Yang F, Wang D, Xing Y, Tsui KL. Prognostics of Li(NiMnCo)O2-based lithium-ion batteries using a novel battery degradation model. Microelectron Reliab 2017;70:70–8.
[23] Dumont O, Dickes R, Lemort V. Extrapolability and limitations of a semi-empirical model for the simulation of volumetric expanders. Energy Procedia 2017;129:315–22.
[24] Cordoba-Arenas A, Onori S, Guezennec Y, Rizzoni G. Capacity and power fade cycle-life model for plug-in hybrid electric vehicle lithium-ion battery cells containing blended spinel and layered-oxide positive electrodes. J Power Sources 2015;278:473–83.
[25] Yang X-G, Leng Y, Zhang G, Ge S, Wang C-Y. Modeling of lithium plating induced aging of lithium-ion batteries: transition from linear to nonlinear aging. J Power Sources 2017;360:28–40.
[26] Pinson MB, Bazant MZ. Theory of SEI formation in rechargeable batteries: capacity fade, accelerated aging and lifetime prediction. J Electrochem Soc 2012;160:A243.
[27] Broussely M, Herreyre S, Biensan P, Kasztejna P, Nechev K, Staniewicz R. Aging mechanism in Li ion cells and calendar life predictions. J Power Sources 2001;97:13–21.
[28] Schmalstieg J, Käbitz S, Ecker M, Sauer DU. A holistic aging model for Li (NiMnCo) O2 based 18650 lithium-ion batteries. J Power Sources 2014;257:325–34.
[29] Han X, Ouyang M, Lu L, Li J. A comparative study of commercial lithium ion battery cycle life in electric vehicle: capacity loss estimation. J Power Sources 2014;268:658–69.
[30] Lin CP, Ling MH, Cabrera J, Yang F, Yu D, Tsui KL. Prognostics for lithium-ion batteries using a two-phase gamma degradation process model. Reliab Eng Syst Saf 2021;214:107797.
[31] Wang J, Meng Z, Wang L. A UPF-PS SLAM Algorithm for indoor mobile robot with non-Gaussian detection model. IEEE/ASME Trans Mechatron 2021;27(1):1–11.
[32] Miao Q, Xie L, Cui H, Liang W, Pecht M. Remaining useful life prediction of lithium-ion battery with unscented particle filter technique. Microelectron Reliab 2013;53:805–10.
[33] Zhang L, Mu Z, Sun C. Remaining useful life prediction for Lithium-ion batteries based on exponential model and particle filter. IEEE Access 2018;6:50587–98.
[34] Walker E, Rayman S, White RE. Comparison of a particle filter and other state estimation methods for prognostics of lithium-ion batteries. J Power Sources 2015;287:1–12.
[35] Rao CR, Rao CR, Statistiker M, Rao CR, Rao CR. Linear statistical inference and its applications. New York: Wiley; 1973.
[36] Arulampalam MS, Maskell S, Gordon N, Clapp T. A tutorial on particle filters for online nonlinear/non-Gaussian Bayesian tracking. IEEE Trans Signal Process 2002;50:174–88.
[37] Yang F, Xing Y, Wang D, Tsui K-L. A comparative study of three model-based algorithms for estimating state-of-charge of lithium-ion batteries under a new combined dynamic loading profile. Appl Energy 2016;164:387–99.
[38] Ng KS, Moo C-S, Chen Y-P, Hsieh Y-C. Enhanced coulomb counting method for estimating state-of-charge and state-of-health of lithium-ion batteries. Appl Energy 2009;86:1506–11.